Anal Bioanal Chem (2009) 393:1123–1133
DOI 10.1007/s00216-008-2489-7

ORIGINAL PAPER

Real-time measurement of endosomal acidification by a novel genetically encoded biosensor

Michela Serresi · Ranieri Bizzarri · Francesco Cardarelli · Fabio Beltram

Received: 1 July 2008 / Revised: 13 October 2008 / Accepted: 16 October 2008 / Published online: 27 November 2008

Abstract Genetically encoded fluorescent proteins are optimal reporters when used to monitor cellular processes as they can be targeted to any subcellular region by fusion to a protein of interest. Here, we present the pH-sensitive fluorescent protein E^{1}GFP which is ideally suited to monitor pH changes in dynamic intracellular structures in real time with high spatio temporal resolution. E^{1}GFP is a ratiometric pH indicator by emission with a pK close to 6.0. We describe an application of this novel pH reporter in the measurement of pH changes along the endo-lysosomal pathway. By fusing E^{1}GFP to the HIV-Tat protein which is endowed with cell-penetrating properties, we were able to monitor multi-step endocytosis from the initial cell-surface binding through to the intracellular endocytic network in real time. This represents a framework for the application of E^{1}GFP to the *in situ* detection of pH changes involved in dynamic biological phenomena.

Keywords Biosensor · Endocytosis · GFP · In vivo imaging · pH measurement · Tat-HIV protein

Electronic supplementary material The online version of this article (doi:10.1007/s00216-008-2489-7) contains supplementary material, which is available to authorized users.

M. Serresi (✉) · R. Bizzarri · F. Cardarelli · F. Beltram
NEST, Scuola Normale Superiore
and Italian Institute of Technology,
Piazza San Silvestro 12,
56124 Pisa, Italy
e-mail: m.serresi@sns.it

R. Bizzarri · F. Cardarelli · F. Beltram
NEST, Scuola Normale Superiore and CNR-INFM,
Piazza San Silvestro 12,
56124 Pisa, Italy

Introduction

Transport of macromolecules from the extracellular milieu to the cell interior is mediated by multiple mechanisms of endocytosis involving carrier vesicles that mature as distinct compartments [1]. A primary function of the endocytic vesicles is to sort internalized cargoes to defined cellular destinations [2]. Besides differences in localization, morphology and dynamics, endosomes also differ in their intraluminal pH [3]. Endosomal acidification represents an essential element of the dynamic progression of organelle contents from endosomes and pinosomes to degradative lysosomal compartments [4]. Monitoring the endocytosis of a macromolecule coming from the external environment in real time by measuring the pH within vesicles can therefore provide useful insight into its intracellular fate. However, the progressive acidification and the fast-moving properties of endocytic vesicles, require non-invasive probes capable of measuring mildly acidic pH values and providing adequate spatio temporal resolution. Fluorophores with pH-dependent properties are ideal candidates for the implementation of such sensors provided they can monitor pH changes with ratiometric properties, in other words their response must not be affected by the concentration of the probe itself [5].

Many organic dyes with pH-dependent optical properties have already been used to determine the pH values of distinct endocytic compartments. Good results were obtained using organic fluorophores such as fluorescein [6, 7]. These approaches, however, require the tagging of small proteins by means of elaborate labeling techniques. Unfortunately, chemical labelling is seldom site specific and this can represent a major obstacle to selective internalization into intracellular organelles. Furthermore, most organic dyes are ratiometric pH indicators by excitation, which means that two excitation wavelengths must be alternated during the measurement. This issue can be better solved by employing

sensors that are ratiometric by emission, i.e., fluorescence excitation by a single monochromatic source and concomitant acquisition at two emission intervals. Here, a beam-splitting device must be used to collect the emission, which is virtually standard in microscopy setups.

pH indicators based on genetically encoded proteins do not require the in vitro labeling procedures associated with the use of organic dyes. In most cases genetically encoded pH indicators represent the best tool, as they can be fused to specific genes and make pH measurement immediate possible with no need for further manipulations. Moreover, through molecular engineering or scanning mutagenesis, it is possible to finely tune indicator properties (subcellular localization [8], p*K*, response dynamic range [5], chloride sensitivity [9]) according to the application of interest. For example, a GFP derivative whose p*K* lies in the alkaline region was recently demonstrated to be an ideal pH indicator for the mitochondrial matrix [10]. Miesenbock and co-workers introduced another family of pH-sensitive GFPs named pHluorins, which are suitable for use as dynamic markers of exocytosis in synaptic transmission [11]. Despite the reported applications, most pH-sensitive GFP mutants possess characteristics of ratiometric indicators by excitation. Remington and coworkers have presented interesting GFP-based pH sensors that are ratiometric by emission (deGFPs) [12]. deGFP4 was successfully used in transfected PS120 cells [12], but its rather weak fluorescence in the lower-wavelength collection range decreases the S/N ratio [13].

In this work we engineered a novel GFP variant (F64L/T203Y GFP, E^1GFP) that displays: 1) a pH- dependent emission wavelength, 2) a p*K* value ideal for mildly-acidic compartments, 3) similar fluorescence in both emission intervals. Moreover, E^1GFP is mostly insensitive to halide ions (e.g. chloride [9]) and is therefore particularly suitable for those subcellular compartments where the lowering of pH is accompanied by an increase in chloride ions (e.g. endocytic vesicles [14]). To assess the ability of E^1GFP to report on the intracellular pH, we focus on real-time monitoring of pH progression during an endo-lysosomal pathway based on HIV-1 Tat intracellular trafficking [15]. HIV-1 Tat protein is a potent transactivator of viral transcription directed by the HIV-1 long terminal repeat (LTR) [16], which possesses an unusual ability to enter cells by endocytosis. As recently reported, Tat enters T-cells using clathrin-coated pits and progressively translocates into well-characterized low-pH endosomes [15]. By using E^1GFP conjugated to Tat we monitored the changes in vesicle pH, starting from the initial cell-surface value through to the intracellular endocytic network, in real time. We demonstrate a progressive acidification within Tat-loaded vesicles that is crucial to the intracellular fate of Tat. The low endosomal pH exploited by Tat-E^1GFP after prolonged incubation in live cells, leads to protein degradation in the lysosomal compartment. We also show that treatment with chloroquine raises the vacuolar pH, demonstrating the ability of E^1GFP to respond effectively to environmental pH changes. We believe that this implementation illustrates the suitability of E^1GFP for use in the surveillance of intracellular pH during dynamic cellular events with high spatio temporal resolution.

Materials and methods

Plasmids and proteins expression

The mammalian expression vector encoding for E^1GFP protein was generated by PCR amplification of EGFP template (Clontech version; Palo Alto, CA, USA) and was inserted into HindIII-EcoRI sites of the pcDNA3.1(+) vector from Invitrogen. Two rounds of site- directed mutagenesis achieved by using the QuickChange Kit (Stratagene, La jolla, CA, USA) according to the manufacturer's instructions, introduced the mutations T65S and T203Y. The primers used for mutagenesis were purchased from Sigma-Genosys (St. Louis, MO, USA). The sequence of sense primer used to mutate the threonine (T) in position 65 to serine (S) was 5′ GTG ACC ACC CTG TCC TAC GGC GTG CAG 3′ while the primer used for the mutation of threonine (T) in position 203 to tyrosine (Y) was 5′ CAA CCA CTA CCT GAG CTA CCA GTC CGC CCT GAG 3′. The antisense primers had the respective reverse complementary sequences. Caveolin-E^1GFP was obtained by PCR amplification of the caveolin-1 sequence starting from the plasmid obtained from L. Pelkmans [17]. The template was introduced into the HindIII-EcoRI sites of pcDNA3.1 in frame with the E^1GFP sequence cloned into the EcoRI-XbaI sites. The ~ 2.9-kb vector pPR-IBA2 (IBA GmbH, Göttingen, Germany) was used for the expression of strep-tagged proteins. The E^1GFP template was cloned into BsaI sites, as described in [9]. The plasmid expressing Tat-E^1GFP was obtained by subcloning the Tat-EGFP fragment derived from pGEX2T-GST-Tat EGFP (described in [18]) into the BamHI and EcoRI sites of the pGEX6P1 vector system (GE Healthcare, Waukesha, WI, USA). The mutant TAT-E^1GFP (T203Y, T65S EGFP) was obtained by substituting the residues at positions 65 and 203 of EGFP by site- directed mutagenesis using the same primer sequences reported above. Expression of recombinant Tat-E^1GFP proteins was induced in the *E. coli* BL21 DE3 strain (Invitrogen) growing in the log phase upon treatment with 1 mM isopropyl-ß-*D*-galactoside at 37 °C 4 h. We used GSTrap HP column (GE Healthcare) for the purification of Tat-E^1GFP by FPLC. A further step to remove the GST tag from Tat-E^1GFP required subsequent treatment with a Prescission™ Protease (GE Healthcare).

Cell culture and transfections

HeLa cells (CCL-2 ATCC) were grown in Dulbecco modified medium (DMEM) supplemented with fetal bovine serum (10%) with glutamine (2 mM), penicillin (10 U/mL) and streptomycin (10 μg/mL), at 37 °C and in a 5% CO_2 atmosphere. Transfections were carried out using lipofectamine reagent (Invitrogen) according to the manufacturer's instructions. For live imaging, 10×10^4 cells were plated 24 hours before the experiments onto a 35-mm glass bottom dish (WillCo-dish GWSt-3522).

Spectroscopy and pH-titration in vitro

Absorption spectra were recorded according to the procedure reported in [5]. Briefly, absorption measurements were done at 23 °C on a Jasco V550 spectrophotometer (JASCO, Easton, MD, USA) by setting the monochromator slits to 2 nm, the scanning speed to 100 nm/min, the data resolution to 0.5 nm, and the time collection average at each wavelength to 0.25 s. Fluorescence measurements were carried out at 23 °C on a Cary Eclipse spectrofluorometer (Varian, Palo Alto, CA) by setting the excitation and emission monochromator slits to 2.5 nm, the scanning speed to 150 nm/min, the data resolution to 0.5 nm, and the time collection average at each wavelength to 0.2 s. Titrations of E^1GFP absorbance and fluorescence versus pH were performed on 2.1 μM protein samples dissolved in a citrate (2 mM)/phosphate (10 mM) buffer with its pH adjusted to the desired value through the addition of 1 M NaOH. In more detail, a concentrated solution of the protein (170 μM) at pH 8.5 (diethanolamine/H_2SO_4 buffer) was added to a previously prepared citrate/phosphate buffer at a certain pH. After the dissolution, the final pH was checked. Given the small volume of protein solution added, the final pH was always within 0.05 pH units of the buffer. Nonetheless, the final pH was used for the titration curve. The extrapolated absorption and fluorescence spectra at pH→-∞ (acid form) and pH→+∞ (alkaline form) were calculated using the ACA method reported in [19]. Fluorescence quantum yields of the protonated forms of E^1GFP were calculated by using quinine sulfate (0.2 N in H_2SO_4) as standard (quantum yields=0.52) and exciting at 380 nm.

pH-titration in living HeLa cells

pH calibrations in living cells were carried out by perfusing HeLa cells transfected with E^1GFP initially for 10 min with an enriched K^+ buffer containing potassium gluconate (120 mM), sodium gluconate (40 mM), HEPES (20 mM), calcium chloride (0.5 mM), and magnesium sulfate (0.5 mM), pH 7.2. Cells were then perfused with the same buffer, adjusted to the desired pH by 0.1 M NaOH, and supplemented with the following compounds: 5 μM nigericin, 5 μM valinomycin, 5 μM carbonyl cyanide *p*-chlorophenyl hydrazone, 10 μM tributyltin chloride, and 20 μM forskolin [20]. Images were taken 10 min after the perfusion with ionophores. Cell imaging data were analyzed using the Leica imaging package (version 2.61) and ImageJ software (NIH Image, http://rsb.info.nih.gov/nih-image/index.html). For the determination of intracellular pH maps, background-subtracted images were processed by the median filter option of the ImageJ software, assuming a pixel radius comparable to the highest achievable optical resolution of the image. A threshold level was determined interactively for each cell.

Internalization assay and biochemical analysis

To monitor Tat-E^1GFP internalization, HeLa cells cultured onto 35-mm glass bottom dishes were incubated with Tat-E^1GFP (0,1–2 μg/mL) in DMEM at 37 °C for 1 h. To remove the unbound proteins in the medium, cells were rinsed three times with cold PBS, with an acid-stripping solution containing ice-cold sodium acetate (0.2 M pH 4.5) and NaCl (0.5 M) for 2 min and 20 s, followed by two rinses with PBS. This acid wash procedure did not affect the internalization properties of HeLa cells [21]. After the initial preloading and subsequent washes, cells were incubated again at 37 °C and analyzed at the indicated time points. For biochemical analysis, HeLa cells were treated with the same protocol described for internalization assay. Cell lysis was performed at the indicated time points as described in [22]. Immunodetections were performed with anti-TAT monoclonal antibody (Advanced Biotechnologies Incorporated), anti-vinculin (Sigma) and with anti-mouse HRP-conjugated secondary antibodies (Amersham Biosciences). A plug-in from ImageJ software (NIH Image, http://rsb.info.nih.gov/nih-image/index.html) has been used to quantify the bands obtained by immunodectection.

Live cell fluorescence microscopy and image analysis

Cell fluorescence was measured using a Leica TCS SP2 inverted confocal microscope (Leica Microsystems AG, Wetzlar, Germany) equipped with an Ar laser for excitation at 488 nm and interfaced with an external diode laser pulsing at 50 MHz (model: C8898 Hamamatsu Photonics Italia, Milan, Italy) for excitation at 403 nm. Glass bottom Petri dishes containing transfected or treated HeLa cells were mounted in a thermostated chamber at 37 °C (Leica Microsystems) and viewed with a 40×1.25 numerical aperture oil immersion objective (Leica Microsystems). The images were collected using low excitation power at the sample (10–20 μW) and the emission was monitored using an acousto-optical beam splitter (AOBS) detection

system on the confocal microscope. The 500–550 nm collection range was adopted for E^1GFP imaging. The ratiometric pH maps of the cells were obtained using emission set up # 1, $F_{505–600}/F_{460–505}$. Image size was 512× 512 pixels and scan speed was usually set to 400 Hz (lines per seconds) corresponding to 0.78 frames per seconds at the resolution used. The pinhole size was set to the optimal value of 1.0 Airy (corresponding to an 81.44-μm confocal aperture). The background signal was subtracted from all images. Vesicle dynamics were recorded by time-lapse experiments at 6.525-s intervals, using the experimental settings described above.

Results

Optical properties of the E^1GFP mutant

The absorption spectrum of the protein contains two main bands in the visible region, one located at 400 nm and one at 510 nm (Fig. 1a). In keeping with the reported spectral properties of GFPs [19], we attributed the first and the second band to the neutral and anionic forms of the chromophore, respectively. Accordingly, raising the pH leads to an increase in the anionic band, but the neutral band does not disappear as expected for a complete interconversion from neutral to anionic chromophores. This result was recently explained by some of us in terms of an additional protonation equilibrium coupled to that of the chromophore [19]. This more complicated protonation pattern does not, however, affect the spectroscopic titration curve of the mutant (Fig. 1b), which revealed a pK of 6.0 when fitted to a single-site binding curve [20]. At pH values below 4.8–5.0, protein unfolding was detected by the appearance of a large band around 370 nm (Fig. 1a).

The fluorescence properties of E^1GFP follows those detected in the absorption spectra. Unlike most GFP variants however, the excitation of the neutral band leads to significant fluorescence emission (Fig. 1c). This effect likely stems from an effective excited-state proton transfer (ESPT) mechanism from the neutral excited state [20]. Remarkably, the modification of the internal protonation regime from low to high pH in E^1GFP yielded two well-separated emission bands from neutral chromophore excitation; the first peaks at 500 nm and the second at 523 nm. The quantum yields of the two emissions were very similar (φ=0.11 for the low pH band, φ=0.15 for the high pH band). The two bands were found to be reversibly interconvertible with pH (Fig. 1c), quantitatively following a single-site titration curve with pK=6.04 (Fig. 1d). The origin of this neutral band splitting is unclear, although we speculate that this effect derives from a different acceptor residue in the ESPT process. Indeed, according to our protonation model, the E222 residue is protonated at low pH and thus cannot act as ESPT acceptor. At pH<5.0, the E^1GFP fluorescence was found to almost disappear, consistently with the protein unfolding process detected from the absorption spectrum.

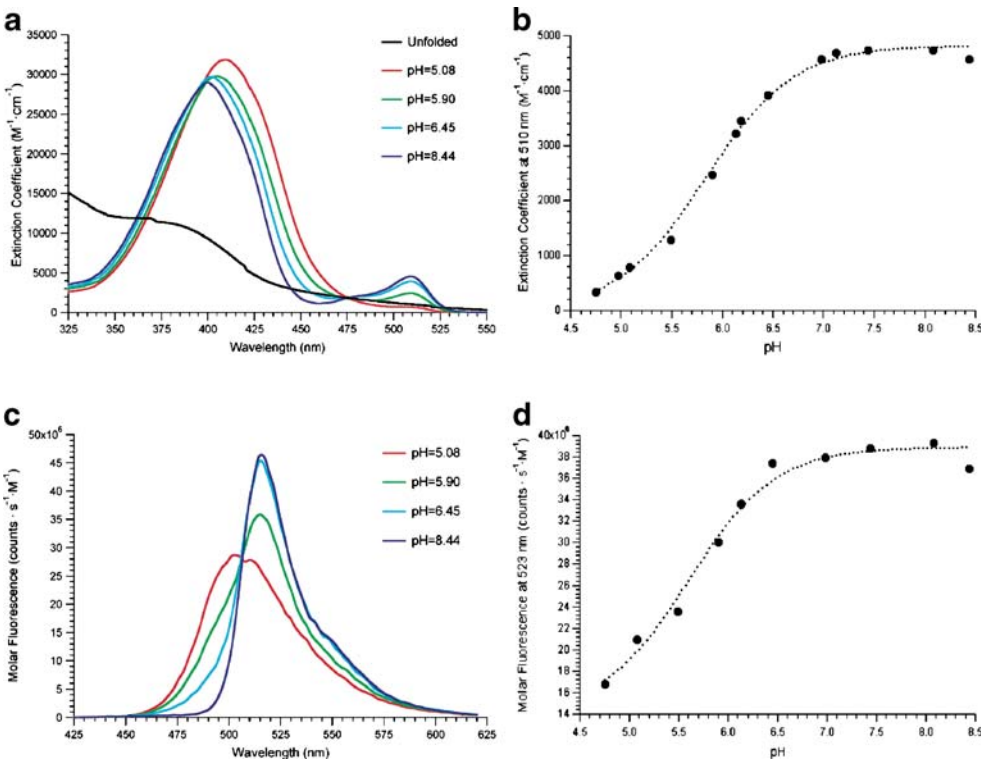

Fig. 1 In vitro spectroscopic properties of E^1GFP. **a** Absorbtion spectra of E^1GFP as a function of pH. **b** In vitro titration of E^1GFP followed by absorbance spectroscopy. **c** Emission fluorescence spectra of E^1GFP at different pH, with excitation at 403 nm. **d** In vitro titration of E^1GFP followed by fluorescence spectroscopy

Emission ratiometric pH indicator properties of E^{1}GFP in vitro

The fairly good quantum yields and large pH-dependent emission shift upon excitation of the neutral form of the chromophore prompted us to evaluate E^{1}GFP as an emission ratiometric pH indicator for intracellular use. The theoretical analysis of ratiometric fluorescent pH indicators shows that the ratio of fluorescence obtained in the two excitation or emission channels (F_1/F_2) has a sigmoidal dependence on pH and is characterized by three parameters, the ratiometric offset (R_0), the dynamic range (R_f), and the ratiometric apparent pK (pK') [5]:

$$\frac{F_1}{F_2} = R_0 \cdot \left(\frac{R_f + 10^{(pK' - pH)}}{1 + 10^{(pK' - pH)}} \right) \quad (1)$$

R_0 is related to the illumination intensities and detection efficiencies; R_f is the dynamic range and depends on the optical characteristics of the fluorescent probes in the detection channels; pK' is the ratiometric (or apparent) pK and is related to the thermodynamic equilibrium pK as well as the optical properties of the protein in channel 2 according to:

$$pK' = pK - \log\left(\frac{F_2^{(pH \to \infty)}}{F_2^{(pH \to -\infty)}} \right) \quad (2)$$

Here, $F_2^{(pH \to +\infty)}$ and $F_2^{(pH \to -\infty)}$ represent the fluorescence collected in channel 2 at very high or very low pH, respectively, for the same concentration of fluorescent probe. Thus, the working range of the pH probe can be adjusted by careful selection of the emission range of channel 2. Note that pK' identifies the linear pH working range of the indicator (≈pK'±1). High R_f values (excellent for high resolution measurements) are often associated with large deviations of pK' from pK. Hence, the collection ranges must be tuned to the pH range where the indicator has to perform its activity, and a compromise between R_f and pK' must be found. The rather low pK of E^{1}GFP makes this protein potentially useful for monitoring mildly- acidic intracellular environments, such as endosomal vesicles. By applying this theoretical approach to experimental fluorescence emission data at different pH values collected during the titration experiments, we identified two ratiometric setups that provide good R_f values along with fairly acidic pK'. Setup #1, $F_{505–600}/F_{460–505}$ (here each subscript refers to the optical collection range in nanometers), yielded R_f=8.57 and pK'=6.68; setup #2, indicated as $F_{510–600}/F_{460–510}$, yielded R_f=4.97 and pK'=6.42. Thus, in both setups the pK' resulted fairly well displaced from the actual pK as a result of higher fluorescence in the $F_{460–505}$ and $F_{460–510}$ channels at low pK compared to high pH (see Eq. 2). Interestingly, shifting the right end of the range from 505 to 510 nm triggered a pK' shift of about 0.25 pH unit. Indeed, the range 505–510 nm is halfway between the emission maximums observed at low and high pH, (Fig. 1b), and a shift of a few nanometers shifts is expected to lead to significant changes in the fluorescence ratio $F_2^{(pH \to +\infty)} \Big/ F_2^{(pH \to -\infty)}$ of Eq. 2.

Emission ratiometric pH indicator properties of E^{1}GFP in living cells

The ratiometric properties of E^{1}GFP were assessed in living cells by an established calibration procedure [20]. HeLa cells were transfected with a vector encoding for E^{1}GFP protein. After 24–48 hours, most cells expressed the protein in the folded fluorescent form, as revealed by confocal microimaging analysis. As expected for a single GFP, E^{1}GFP was found to be uniformly distributed in the cell [23]. Cells were then perfused at 37 °C with buffers at different pH values (5.5–8.0) containing a mixture of ionophores in order to clamp the intracellular pH to the extracellular value (Fig. 2a). Spectral detection of intracellular fluorescence was carried out by exciting the neutral protein chromophore at 403 nm using a laser source interfaced with the confocal microscope. In accordance with our in vitro determination, we collected the fluorescence signals in the four wavelength ranges (460–505), (505–600), (460–510), and (510–600) to evaluate the ratiometric response in setup #1 and #2. Plots of the $F_{505–600}/F_{460–505}$ (setup #1) and $F_{510–600}/F_{460–510}$ (setup #2) ratios *versus* pH are reported in Fig. 2b. Fitting the ratiometric curves using Eq. 1 yielded R_f=8.4 and pK'=6.65 for $F_{505–600}/F_{460–505}$, and R_f=5.09 and pK'=6.40, in excellent agreement with the in vitro data. Such an agreement provides indirect evidence that the cellular environment does not affect significantly the pK (and, in turn, pK') of E^{1}GFP. Indeed, solution parameters such as the ionic strength, which are known to strongly modulate the pK values of most acidic compounds have been found to be much less significant when determining the protonation of the GFP chromophore, due to the protective effect of the protein structure [24].

As a first assessment of E^{1}GFP's ability to monitor pH during dynamic cellular events, we constructed a C-terminally-tagged caveolin-E^{1}GFP fusion protein. Caveolin-1 is a key component of caveolar membrane which has the N and C termini facing the cytoplasm and a putative "hairpin" intramembrane domain embedded within the membrane bilayer [25]. When the C- terminus of caveolin is fused to GFP, the resulting fusion protein is known to yield both a dotted staining at the plasma membrane, corresponding to a highly immobile cluster of membrane-caveolae, and cytoplasmic structures concentrated in the perinuclear region that showed rapid movements [26].

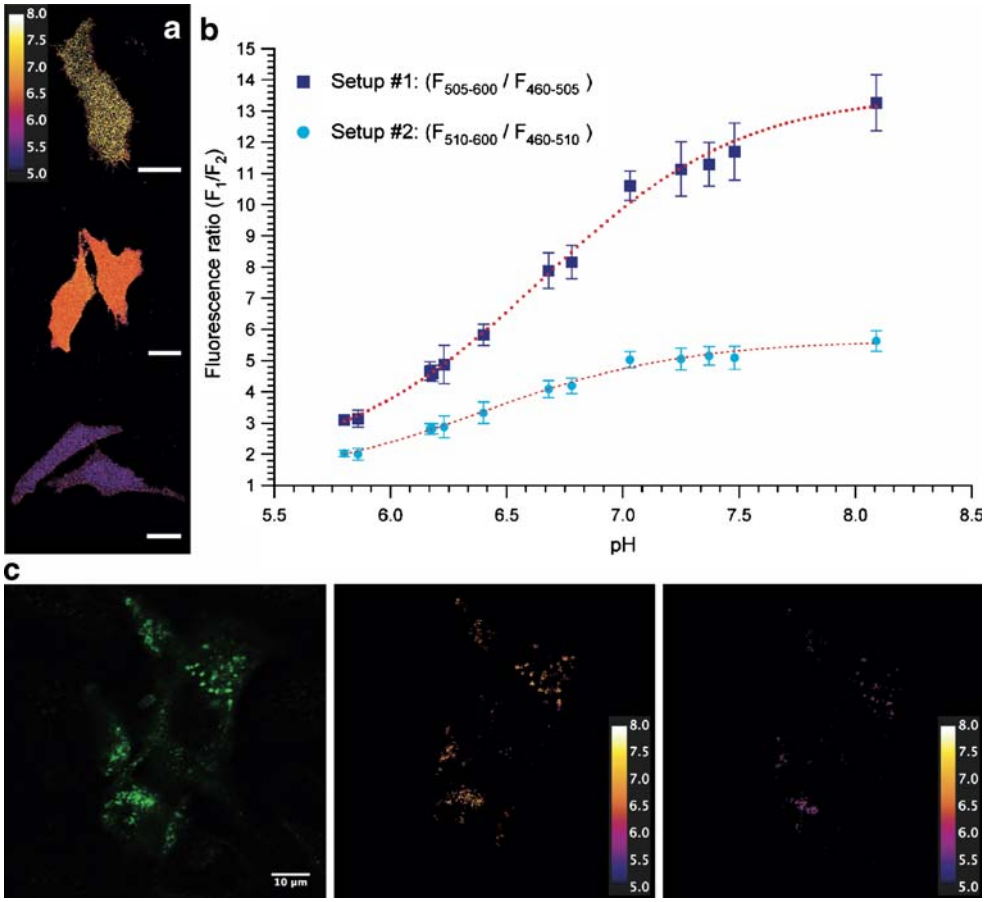

Fig. 2 Ratiometric calibration of E[1]GFP (excitation at 403 nm) in living cells. **a** Ratiometric pH-map by emission in single HeLa cells clamped at different pH values: pH 8 (*upper panel*) pH 6.7 (*middle panel*) pH 5 (*lower panel*). Images are color-encoded according to the look-up table on the left. Scale bar represents 10 μm. **b** Ratiometric calibration curves of E[1]GFP in living HeLa cells clamped at different pH values. The *blue squares* refer to the $F_{505–600}/F_{460–505}$ ratio (emission setup #1), whereas the *cyan circles* refer to the ($F_{510–600}/F_{460–510}$) ratio (emission setup #2); *dashed curves* represent fits of achieved using Eq. 1. **c** Confocal imaging of a single HeLa cell transfected with caveolin-E[1]GFP (*left panel*). Ratiometric pH- map by emission (setup# 1) of cytosol under physiological conditions: pH 7.3± 0.2 (*middle panel*). The same cell was analyzed after treatment with HEPES buffer supplemented with ionophores and after perfusion of permeant acid to clamp intracellular pH to 5 (*right panel*)

We used the intracellular pool of caveolin as a dynamic enclosed-membrane compartment that exposed E[1]GFP to the cytosol. Caveolin-E[1]GFP- transfected cells were readily observed by confocal microscopy under both the $F_{505–600}/F_{460–505}$ and $F_{510–600}/F_{460–510}$ setups. From the calibration curves, we determined that the cytosol has a pH of 7.3±0.2 (Fig. 2c middle panel) in agreement with previously published data [27]. To demonstrate that dynamic measurements of acidic pH values were equally feasible, we clamped the intracellular pH of the transfected cells to 5.5. After 5 min of acidic treatment in the same Petri dish, caveolin-E[1]GFP was found to respond in accordance with the cytoplasm pH decrease (Fig. 2c, right panel). Taken together, these data show that our approach can be applied in order to measure pH changes in dynamic structures inside a living cell.

From the plasmamembrane to the endosomal-lysosomal pathway: real-time monitoring of endosomal acidification in Tat- E[1]GFP- loaded vesicles

To assess the ability of E[1]GFP to measure the pH of dynamic endocytic organelles, we monitored the progressive endosomal acidification during Tat HIV-1 intracellular trafficking. As a first step, we engineered a recombinant fusion protein where the full-length cDNA of E[1]GFP was fused to the C- terminus of the Tat sequence. The expected size of the purified product, ca. 39 kDa, was confirmed by Western blotting using a mouse monoclonal antibody directed against Tat protein. To monitor Tat endocytosis, HeLa cells were preloaded with Tat E[1]GFP for 1 h at 37 °C (concentrations ranging from 10–50 nM). Consistent with previous reports [15], our analysis confirmed that the

overall process of endocytosis was very slow. Indeed, we found that, immediately after pre- binding, Tat- cargoes accumulated in bright patches on the plasma membrane. However, only 4 h later, one or a few clusters of vesicles embedded in the cytoplasm (Fig. 3a; see magnification in Fig. 3c). The fast-moving behavior of the Tat-E^{1}GFP intracellular pool was assessed by time-lapse experiments (see the movie in Electronic Supplementary Material). Vesicles rapidly moved into the intracellular environment, and they frequently interacted with each other in a "kiss-and-run" fashion [28]. By using the calibration setups described previously, we were able to determine the pH of Tat-loaded endosomes (Fig. 3b). Vesicles that were localized close to the plasma membrane showed a pH value of 6.77±0.13 (*cells*=15). In the internalized pool (*cells*=15; *vesicles*=225) we identified two subpopulations of endosomes characterized by different pH values: 6.52 (σ=0.11) and 5.95 (σ=0.17) (Fig. 3e). After a further 2 h, we

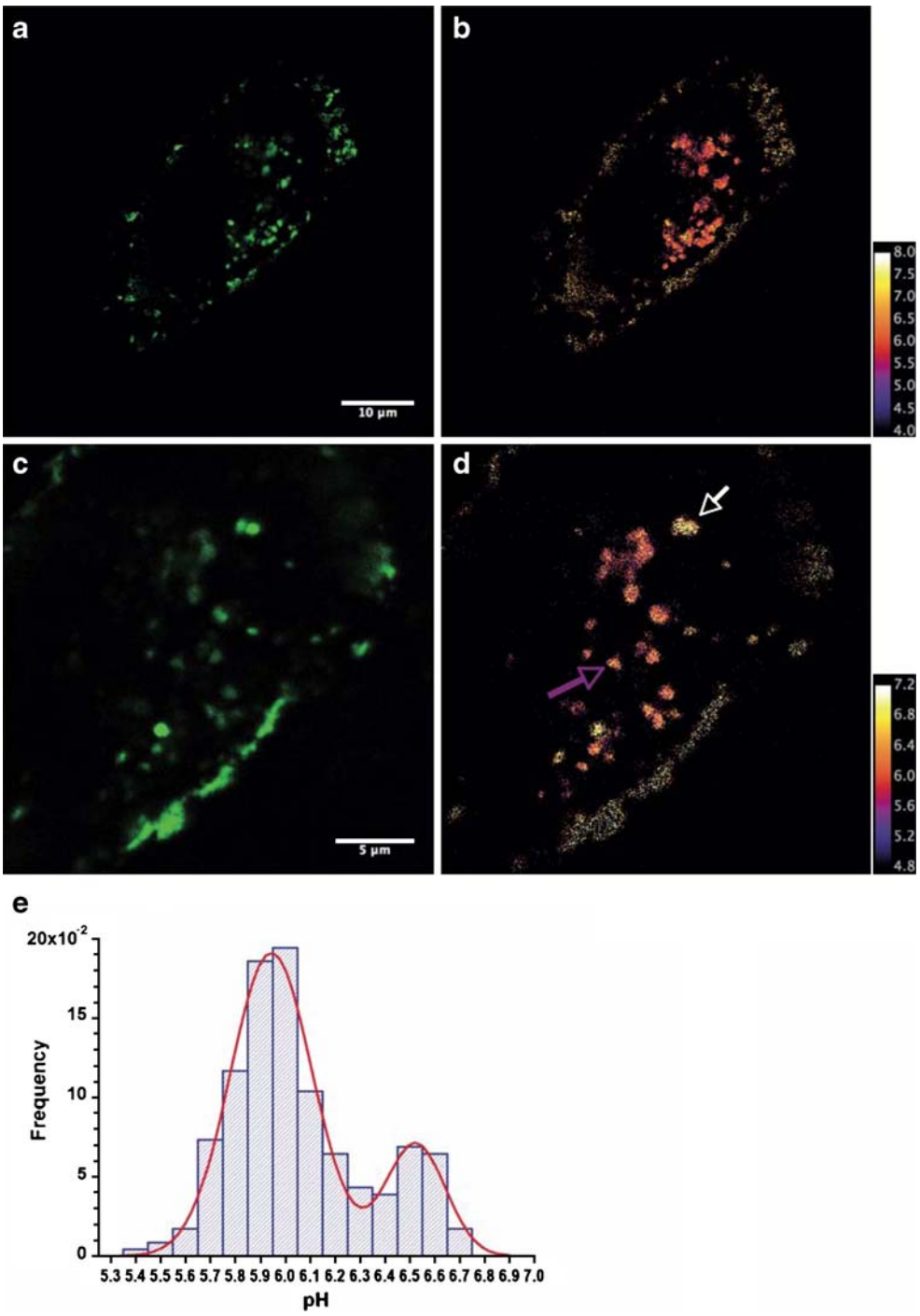

Fig. 3 Measurement of endosomal acidification after 4 h of Tat-E^{1}GFP endocytosis. **a** Four hours after treatment with Tat-E^{1}GFP, the HeLa cells were visualized for E^{1}GFP fluorescence (*green*) **b** Ratiometric pH map of Tat-E^{1}GFP-loaded vesicles. Image is color-coded according to the look-up table on the *right*. Magnified area of the same cell is shown in **c** (fluorescence signal) and **d** (ratiometric pH map). Arrows in **d** indicate two endosomes belonging to the two identified subpopulations: *white arrow* vesicle pH=6.58, *purple arrow* vesicle pH=5.79. **e** pH distribution of Tat-E^{1}GFP intracellular vesicles. After 4 h of endocytosis the intracellular pool (*cells*=15; *vesicles*=225) was composed by two subpopulations of endosomes pH=6.52 (σ=0.11) and pH=5.95 (σ=0.17)

observed a clear modification in terms of both endosomes localization (Fig. 4a; see magnification in Fig. 4c) and pH of vesicles (Fig. 4b; see magnification in Fig. 4d). In detail, endosomes localized close to the membrane showed a pH value of 6.31±0.2 (*cells*=15) whereas the internalized pool (*cells*=15; *vesicles*=122) that accumulated in the perinuclear area showed a single pH value of 5.83 (σ=0.14) (Fig. 4e).

Thus, the Tat-E^{1}GFP indicator demonstrated that during endocytosis Tat underwent low-endosomal pH changes, moving from mildly acidic endosomes to more acidic compartments that are well recognized as the final destination for macromolecules degradation. This progressive acidification prompted us to investigate the stability of Tat-E^{1}GFP during endocytosis and its intracellular fate. HeLa cells were preloaded with Tat-E^{1}GFP for 1 h. To remove the excess of unbound Tat-E^{1}GFP, HeLa cells were washed and then incubated again for a further 2, 4, 6, 8 and 24 h. In order to detect any decrease in the amount of Tat protein at the indicated time points, we performed cell lysis and immunoblot detection by using an antibody directed

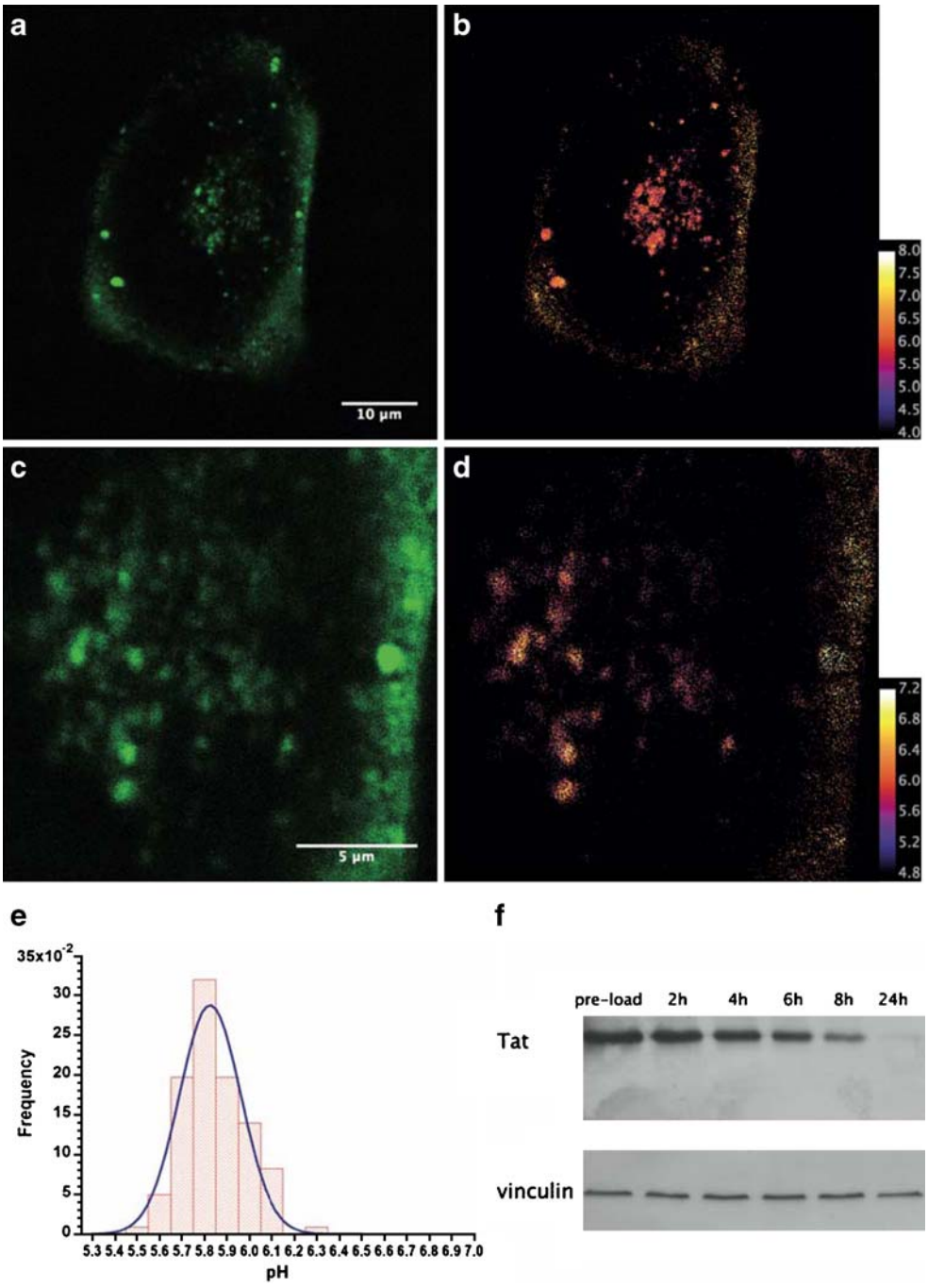

Fig. 4 Measurements of vesicle pH changes after 6 h of Tat-E^{1}GFP internalization. **a** Confocal image of HeLa cell treated with Tat-E^{1}GFP for 6 h. **b** Ratiometric pH-map of Tat-E^{1}GFP-loaded vesicles. Magnified area of the same cell is shown in **c** (fluorescence signal) and **d** (ratiometric pH-map). **e** pH distribution of endosomes and Gaussian fit after 6 h of Tat-E^{1}GFP endocytosis. The histogram show one population of intracellular vesicles (*cells*=15; *vesicles*=122) with an average pH value of 5.83 (σ=0.14). **f** Analysis of Tat-E^{1}GFP stability during internalization. HeLa cells were preloaded with Tat-E^{1}GFP for 1 h at 37 °C. Then the cells were washed with an acidic buffer (pH=4.5) and incubated at 37 °C for the indicated time points. Cells lysis was performed at 2, 4, 6, 8 and 24 h after incubation. To determine the level of Tat-E^{1}GFP protein an immunodetection using antibodies directed against Tat was performed

against Tat protein. Our results showed that the intracellular levels of Tat-E^{1}GFP remained constant during the first 6 h of uptake but declined at 8 h (about 40% lower than the amount of protein at 6 h and 70% lower than the initial preloading), eventually disappearing after 24 hours (Fig. 4f).

Effect of chloroquine- treatment on the neutralization of low-endosomal pH

The lysosome is the final destination of many macromolecules internalized by the endo-lysosomal pathway and is characterized by a strongly acidic pH [29]. As previously reported, acidic conditions lead to quenching and irreversible unfolding of GFP proteins [30]. Indeed, imaging analysis performed after 10 h of endocytosis showed a dramatic decrease in the intracellular Tat-E^{1}GFP fluorescence, although many signals were detected close to the membrane (Fig. 5a). These results are in keeping with the final localization of Tat-E^{1}GFP in lysosomal compartments [15]. To better investigate this point, we carried out the internalization experiment in the presence of chloroquine, a well-recognized lysomotropic agent that raises the intra-lysosomal pH and specifically blocks lysosomal degradation. As expected, at 10 h of Tat internalization and upon chloroquine treatment we observed enhanced vesicular staining (Fig. 5b,c). The ratiometric pH map of Tat-E^{1}GFP- loaded vesicles showed a homogenous distribution of pH within endosomes of 6.2±0.2 (Fig. 5d). Overall, these experiments reveal a possible protecting role of chloroquine on Tat degradation within lysosomes.

Discussion

The aim of this work was to demonstrate the capabilities of a novel GFP-based fluorescent probe of high-resolution pH measurements in living cells. This probe was put to the test by investigating HIV-1 Tat protein internalization in real time.

Our GFP variant (E^{1}GFP) is characterized by the F64L and T203Y mutations and belongs to the family of yellow fluorescent proteins. Compared to other GFP mutants, this probe offers the following properties: (i) its pK is close to 6.0 and it is therefore particularly suitable for pH detection below neutrality; (ii) upon excitation of the neutral state of the chromophore (~400–410 nm), the emission properties of E^{1}GFP are strongly dependent on the environmental pH.

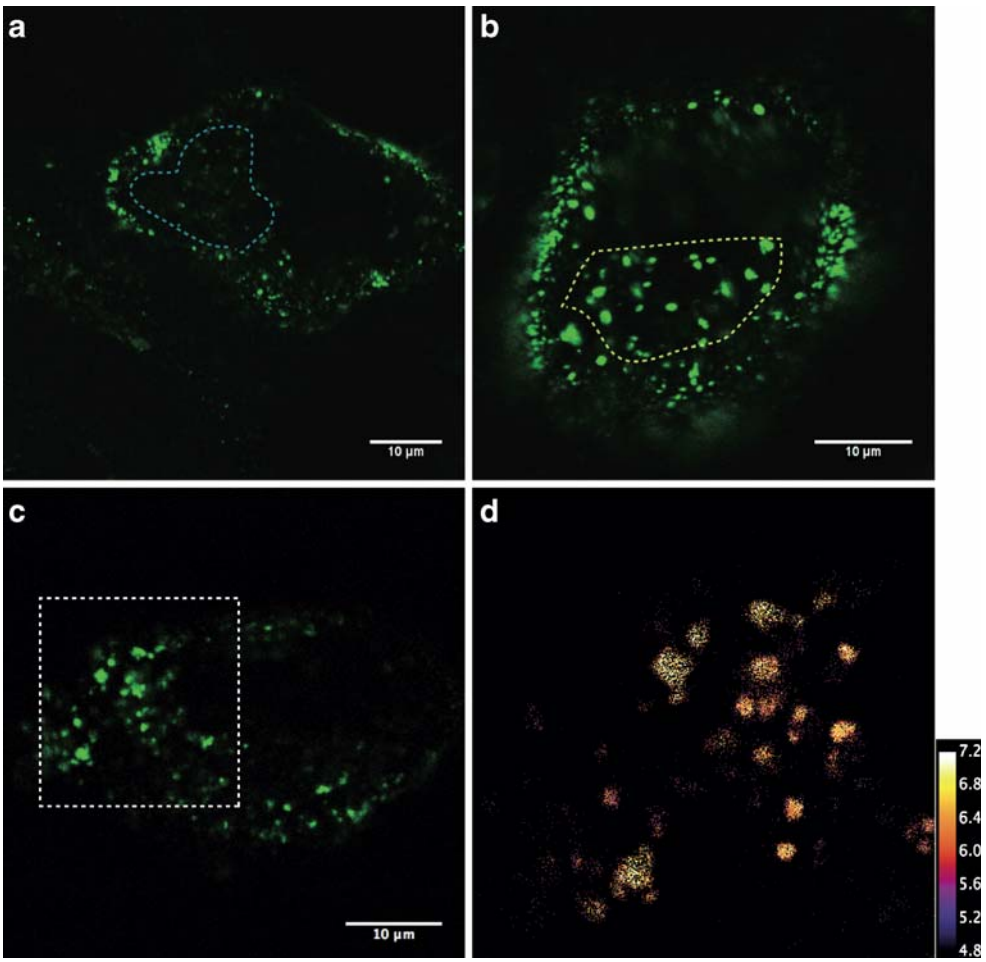

Fig. 5 Effects of chloroquine treatment on endosomal- pH. **a** After 10 h of internalization the intracellular fluorescence signal of Tat-E^{1}GFP- loaded-vesicles dramatically disappeared (*blue dashed box*). **b** At the same time point HeLa cells treated with chloroquine displayed an enhanced intracellular vesicle-associated staining (*yellow dashed box*). **c** Fluorescence image of Tat- E^{1}GFP loaded-vesicles in the presence of chloroquine. *White dashed box* represents the magnification of the area indicated in **d**. **d** Ratiometric pH-map of Tat-E^{1}GFP signal shows a homogenous distribution of pH within endosomes of approximately 6.2. Scale bar represents 2 µm

This latter characteristic is the basis of pH measurements by emission with ratiometric characteristics. Indeed, we identified two emission intervals for ratiometric image acquisition ($F_{505–600}/F_{460–505}$ and $F_{510–600}/F_{460–510}$), which provide a rather high dynamic range of response, and we calculated a ratiometric pK' between 6.4 and 6.7. Additionally, the good emission of E^1GFP in both collection channels ensures that a good signal to noise ratio is always achieved and therefore small pH changes can be monitored in a reliable way.

The ratiometric by emission characteristics of E^1GFP make this reporter a pH-indicator that is ideally suited for detecting pH changes within highly dynamic compartments as occurring in a wide range of cellular processes. In the endo-lysosomal pathway, the acidic nature of endosomes is directly responsible for the sorting and processing of internalized molecules right up to their final compartment destination and subsequent degradation [31]. Nowadays, biochemical and molecular biology techniques represent powerful tools in the identification of intracellular routes of internalized molecules [32]. They cannot report however, on the progressive acidification of vesicles, which is a crucial process for understanding the intracellular fate of exogenous molecules upon internalization.

As paradigm of endocytosis, we focused on HIV-1 Trans-activating (Tat) viral protein intracellular trafficking. In keeping with the expected Tat behavior [15], Tat-E^1GFP internalization was found to follow a multi-step mechanism. The purified protein added to a culture medium first attached to the cell membranes - presumably by ionic interactions - and then it was entrapped within vesicle-like structures. During internalization, we observed that Tat-E^1GFP accumulated in two distinct intracellular domains: one close to the plasmamembrane and the second embedded in the cytoplasm. After 4 h the vesicles associated with the membrane showed a nearly neutral pH (6.77) whereas after two more hours the pH decreased to a mean value of 6.31. Significantly, it was recently reported that early endosomes comprise two distinct populations: a dynamic pool that is highly mobile on microtubules and rapidly evolving towards late endosomes, and a more static one that is close to the membrane that matures much more slowly [33]. Furthermore, among the membrane vesicles there are also the recycling compartments characterized by mildly acidic luminal pH. The decrease in the pH observed 6 h later is also probably due to the presence of the Tat-E^1GFP recycling pool. Recycling endosomes undergo further rounds of internalization and they are not involved in degradation. As for the intracellular dynamic vesicles, after 4 h we identified two distinct endosomal subpopulations characterized by different average pH values: 6.52 and 5.95, respectively (Fig. 3e). The slightly more acidic unique pH=5.83 observed at 6 h (Fig. 4e) suggests that, with time, these two pools matured into a single one. Studies performed in T cells by Vaudeville and coworkers are perfectly in keeping with our results; they indicated that upon internalization, Tat concentrated within early endosomes at 3 h, whereas after 6 h it colocalized with late endosome/lysosome markers [15]. The eventual uptake by the lysosomal compartment could not be observed in our experiments owing to the much more acidic pH that triggered protein degradation (Fig. 4f). The addition of chloroquine (a lysomotrophic agent) raised the pH of the vesicles to 6.2, delaying Tat-E^1GFP degradation for up to 10 h. Previous works by Frankel and Pabo demonstrated that in HeLa cells the transactivation of the viral promoter induced by Tat is dramatically increased by a variety of lysosomotrophic agents, such as chloroquine. In our system, we show that the chloroquine treatment leads to enhanced intracellular vesicles staining corresponding to a homogeneous Tat-vesicle population with a mildly acidic pH (approximately 6.2). This may favor the escape of Tat into the cytosol and subsequent translocation into the nucleus and in turn explain the high level of transactivation reported in the presence of chloroquine [34].

In addition, in confirming of the intracellular endocytic pathway followed by Tat (achieved by monitoring endosomal pH), this work represents a proof of the functionality of E^1GFP as a pH indicator that is potentially applicable in dynamic membrane-enclosed compartments. By taking advantage of the E^1GFP-based sensor efficiency, a wide range of biological processes involving changes in the pH gradient (cell polarity, migration, intracellular transport of drugs, penetration of cytosol by certain enveloped viruses) can be monitored in real time with high spatio-temporal resolution.

Conclusion

It is well established that intracellular pH (pH_i) plays a pivotal role as a modulator of cell function. Many cellular mechanisms are influenced by pH_i changes including cell metabolism, gene expression, organelle functions and cell death. In particular, the maintenance of an appropriate pH within intracellular membrane-enclosed compartments is essential for many biological processes and any aberration of intraorganelle pH homeostasis can lead to significant functional changes. Therefore monitoring pH_i with high spatial resolution can help to elucidate many physiological or pathogenic processes taking place within cells.

In this report, we describe a new method for monitoring pH changes during dynamic cellular events in living cells. To this aim, we engineered a novel variant of green fluorescent protein (F64L T203Y GFP) that is suitable for ratiometric emission measurements in living cells. The use of E^1GFP as a genetically encoded biosensor is associated

with several advantages. E^1GFP is capable of measuring pH within specific intracellular regions with little background signal and without the need for invasive loading procedures. Additionally, neither probe leakage nor the toxicity associated with the use of many chemical probes is observed when E^1GFP is applied in living cells. The E^1GFP probe shows rapid signal response to pH changes and good luminescent/optical properties. Given its favourable optical characteristics, its p*K* which is suitable to address the mildly-acidic/physiological pH ranges, and its suitability for ratiometric measurements, E^1GFP should make an excellent probe for studying real-time changes of pH in living cells. The extension of the emission ratiometric properties of E^1GFP to two-photon excitation cell imaging and its application in order to shed light on relevant biological processes involving pH changes will be the tasks of forthcoming studies.

Acknowledgments We thank Dr. Stefano Luin (Scuola Normale Superiore) for the expert technical assistance and helpful in discussion. The authors also gratefully acknowledge partial the financial support of the Italian Ministry for University and Research (FIRB No. RBLA03ER38) and of the Fondazione Monte dei Paschi di Siena.

References

1. Gruenberg J (2001) Nat Rev Mol Cell Biol 2:721–730
2. Mellman I, Warren G (2000) Cell 100:99–112
3. Fuchs R, Schmid S, Mellman I (1989) Proc Natl Acad Sci USA 86:539–543
4. Gruenberg J, Stenmark H (2004) Nat Rev Mol Cell Biol 5:317–323
5. Bizzarri R, Arcangeli C, Arosio D, Ricci F, Faraci P, Cardarelli F, Beltram F (2006) Biophys J 90:3300–3314
6. Gagescu R, Demaurex N, Parton RG, Hunziker W, Huber LA, Gruenberg J (2000) Mol Biol Cell 11:2775–2791
7. Bache KG, Stuffers S, Malerod L, Slagsvold T, Raiborg C, Lechardeur D, Walchli S, Lukacs GL, Brech A, Stenmark H (2006) Mol Biol Cell 17:2513–2523
8. Cardarelli F, Serresi M, Bizzarri R, Beltram F (2008) Traffic 9:528–539
9. Arosio D, Garau G, Ricci F, Marchetti L, Bizzarri R, Nifosi' R, Beltram F (2007) Biophys J 93(932):944
10. Abad MF, Di Benedetto G, Magalhaes PJ, Filippin L, Pozzan T (2004) J Biol Chem 279:11521–11529
11. Miesenbock G, De Angelis DA, Rothman JE (1998) Nature 394:192–195
12. Hanson GT, McAnaney TB, Park ES, Rendell ME, Yarbrough DK, Chu S, Xi L, Boxer SG, Montrose MH, Remington SJ (2002) Biochemistry 41:15477–15488
13. McAnaney TB, Park ES, Hanson GT, Remington SJ, Boxer SG (2002) Biochemistry 41:15489–15494
14. Jentsch TJ (2007) Phisiol J 578:633–640
15. Vendeville A, Rayne F, Bonhoure A, Bettache N, Montcourrier P, Beaumelle B (2004) Mol Biol Cell 15:2347–2360
16. Raha T, Cheng SW, Green MR (2005) PLos Biol 3:e44
17. Pelkmans L, Kartenbeck J, Helenius A (2001) Nat Cell Biol 3:473–483
18. Tyagi M, Rusnati M, Presta M, Giacca M (2001) J Biol Chem 276:3254–3261
19. Bizzarri R, Nifosi R, Abbruzzetti S, Rocchia W, Guidi S, Arosio D, Garau G, Campanini B, Grandi E, Ricci F, Viappiani C, Beltram F (2007) Biochemistry 46:5494–5504
20. Jayaraman S, Haggie P, Wachter RM, Remington SJ, Verkman AS (2000) J Biol Chem 275:6047–6050
21. Serresi M, Piccinini G, Pierpaoli E, Fazioli F (2004) Oncogene 23:1098–1108
22. Piccinini G, Bacchiocchi R, Serresi M, Vivani C, Rossetti S, Gennaretti C, Carbonari D, Fazioli F (2007) J Biol Chem 277:22231–22239
23. Cardarelli F, Serresi M, Bizzarri R, Giacca M, Beltram F (2007) Mol Ther 15:1313–1322
24. Haupts U, Maiti S, Schwille P, Webb WW (1998) Proc Natl Acad Sci USA 95:13573–13578
25. Parton RG, Simons K (2007) Nat Rev Mol Cell Biol 8:185–194
26. Thomsen P, Roepstorff K, Stahlhut M, van Deurs B (2002) Mol Biol Cell 13:238–250
27. Llopis J, McCaffery JM, Miyawaki A, Farquhar MG, Tsien RY (1998) Proc Natl Acad Sci USA 95:6803–6808
28. Bright NA, Gratian MJ, Luzio JP (2005) Curr Biol 15:360–365
29. Fasen K, Cerretti DP, Huynh-Do U (2008) Traffic 9:251–266
30. Kneen M, Farinas J, Li Y, Verkman AS (1998) Biophys J 74:1591–1599
31. Luzio JP, Pryor PR, Bright NA (2007) Nat Rev Mol Cell Biol 8:622–632
32. Zuccato E, Blott EJ, Holt O, Sigismund S, Shaw M, Bossi G, Griffiths GM (2007) J Cell Sci 120:191–199
33. Lakadamyali M, Rust MJ, Zhuang X (2006) Cell 124:997–1009
34. Frankel AD, Pabo CO (1988) Cell 55:1189–1193